Statistical Properties Of Turbulent Rayleigh-Bénard Convection

Westfälische Wilhelms-Universität Münster
institute for theoretical physics

J. Lülff
M. Wilczek
R. Friedrich

johannes.luelff@uni-muenster.de
mwilczek@uni-muenster.de
fiddir@uni-muenster.de

Introduction

- Rayleigh-Bénard convection is the buoyancy-driven flow of a fluid enclosed between two horizontal plates.
- We investigate statistical properties of different fluctuating quantities like temperature and velocity in the turbulent regime, i.e. at high Rayleigh number.
- For this, we make use of the Lundgren-Monin-Novikov hierarchy and derive equations determining the probability density functions (PDFs).
- Direct numerical simulation (DNS) of the basic equations governing the flow is used to obtain the statistical quantities.
- The numerical scheme makes use of volume penalization to model the boundaries, i.e. horizontal plates.

Governing Equations

- The nondimensionalized equations governing the Rayleigh-Bénard system in Oberbeck-Boussinesq approximation read

$$\frac{\partial}{\partial t}\boldsymbol{u}+\boldsymbol{u}\cdot\nabla\boldsymbol{u}=-\nabla p+\mathrm{Pr}\Delta\boldsymbol{u}+\mathrm{Pr}\,\mathrm{Ra}\,T\boldsymbol{e}_z,\quad \nabla\cdot\boldsymbol{u}=0$$
$$\frac{\partial}{\partial t}T+\boldsymbol{u}\cdot\nabla T=\Delta T \tag{1}$$

with the velocity field $\boldsymbol{u}(\boldsymbol{x},t)$, the temperature field $T(\boldsymbol{x},t)$ and the pressure field $p(\boldsymbol{x},t)$.
- The nondimensional control parameters are the Rayleigh number Ra, the Prandtl number Pr and the aspect ratio Γ

$$\mathrm{Ra}=\frac{\alpha g\,\delta T h^3}{\nu\kappa}$$
$$\mathrm{Pr}={}^{\nu}/_{\kappa}$$
$$\Gamma={}^{L_x}/_{h}$$

with thermal expansion coefficient α, gravitational acceleration g, outer temperature difference δT, vertical distance of top and bottom plate h, horizontal size L_x, kinematic viscosity ν and heat conductivity κ.
- The spatial domain is $\Omega=[0,\Gamma]\times[0,\Gamma]\times[0,1]$ and is periodic in horizontal direction. Boundary conditions in vertical direction are

$$\boldsymbol{u}(z=0)=\boldsymbol{u}(z=1)=0$$
$$T(z=0)={}^{1}/_{2}$$
$$T(z=1)=-{}^{1}/_{2}$$

3D Direct Numerical Simulation

- For convenience, we use the Oberbeck-Boussinesq-equations that have not been nondimensionalized.
- We use a pseudospectral scheme in the variables *vorticity* $\boldsymbol{\omega}(\boldsymbol{x},t)=\nabla\times\boldsymbol{u}(\boldsymbol{x},t)$ and *deviation from the linear temperature profile* $\theta(\boldsymbol{x},t)=T(\boldsymbol{x},t)+\frac{\delta T}{h}\left(z-\frac{h}{2}\right)$; therefore, boundary conditions are $\theta(z=0)=\theta(z=h)=0$.
- The boundary conditions in vertical direction are enforced by volume penalization [1,2], i.e. an immersed boundary method where a strong exponential damping acting on $\boldsymbol{u}$ and θ models a porous medium of constant temperature.
- The equations are formulated for $\tilde{\boldsymbol{\omega}}(\boldsymbol{k},t)=\mathscr{F}[\boldsymbol{\omega}]$ and $\tilde{\theta}(\boldsymbol{k},t)=\mathscr{F}[\theta]$ in Fourier space:

$$\frac{\partial}{\partial t}\tilde{\boldsymbol{\omega}}=i\boldsymbol{k}\times\mathscr{F}\left[\mathscr{F}^{-1}[\tilde{\boldsymbol{u}}]\times\mathscr{F}^{-1}[\tilde{\boldsymbol{\omega}}]-\frac{1}{\eta}\chi\cdot\mathscr{F}^{-1}[\tilde{\boldsymbol{u}}]\right]-\nu k^2\tilde{\boldsymbol{\omega}}+\alpha g i\boldsymbol{k}\times\left(\tilde{\theta}\boldsymbol{e}_z\right)$$
$$\frac{\partial}{\partial t}\tilde{\theta}=-\mathscr{F}\left[\mathscr{F}^{-1}[\tilde{\boldsymbol{u}}]\cdot\mathscr{F}^{-1}\left[i\boldsymbol{k}\tilde{\theta}\right]-\frac{1}{\eta}\chi\cdot\mathscr{F}^{-1}\left[\tilde{\theta}\right]\right]-\kappa k^2\tilde{\theta}+\frac{\delta T}{h}\tilde{u}_z \tag{2}$$

The red terms correspond to the volume penalization terms with the masking function $\chi=\chi(\boldsymbol{x})\in\{0,1\}$ that separates fluid and porous/solid domains and the penalization parameter $\eta\ll1$.
- The numerically expensive convolution in complex space that would arise from the nonlinearity is avoided by switching back to real space.
- Aliasing errors stemming from the nonlinearity are handled via a smooth Fourier filter [3].
- Time stepping of (2) is done via a 3rd order Runge-Kutta-scheme [4] that handles the diffusion terms implicitly via an integrating factor technique.
- The simulation code is MPI-parallelized using slab decomposition and a parallel version of the free Fast Fourier Transform library FFTW2 [5].
- The scheme can be extended to include vertical no-flux walls of arbitrary shape, cf. [6,7].

Visualization Of Temperature Field

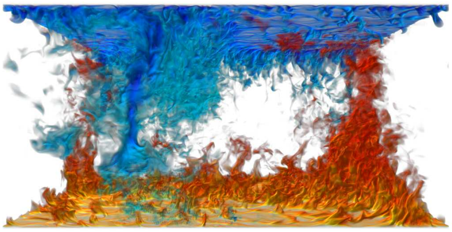

Volume rendering of a temperature field at parameters $\mathrm{Ra}=10^9$, $\mathrm{Pr}=1$ and $\Gamma=2$. Red corresponds to hot, blue to cold parts of the fluid. The volume rendering is done with the free volume rendering engine Voreen [8], developed at the University of Münster.

Statistics And Symmetries

- The system has axial symmetry, i.e. turbulence is homogeneous and isotropic in x- and y-direction. Furthermore, it is stationary in time.
- Therefore, averaged quantities, e.g. the probability density function of velocity $\boldsymbol{v}$, only depend on z, that is $f(\boldsymbol{v};\boldsymbol{x},t)=f(\boldsymbol{v};z)$
- In axial symmetry, an isotropic vector quantity $\boldsymbol{a}(\boldsymbol{v})$ can be expressed as

$$\boldsymbol{a}(\boldsymbol{v})=a_h(v_h,v_z)\,\hat{\boldsymbol{v}}_h\;+\;a_z(v_h,v_z)\,\hat{\boldsymbol{v}}_z\;+\;a_\varphi(v_h,v_z)\,\hat{\boldsymbol{v}}_\varphi$$

with $\hat{\boldsymbol{v}}_h$, $\hat{\boldsymbol{v}}_z$ and $\hat{\boldsymbol{v}}_\varphi=\hat{\boldsymbol{v}}_h\times\hat{\boldsymbol{v}}_z$ being unit vectors in horizontal, vertical and azimuthal direction, respectively (cf. [9]).
- Symmetry considerations allow us to express the PDF $\tilde{f}(v_h,v_z;z)$ of the horizontal and vertical velocity in terms of the PDF $f(\boldsymbol{v};z)$ of the full velocity vector:

$$\tilde{f}(v_h,v_z;z)=2\pi v_h f(\boldsymbol{v};z)$$

Deriving Evolution Equations For PDFs

- Within the framework of the LMN hierarchy [10,11,12], one can derive evolution equations for PDFs from first principles. This will be exemplified for the joint PDF of temperature and velocity, following the steps suggested in [13].
- The basic idea is to define a fine-grained PDF $\hat{f}(\tau,\boldsymbol{v};\boldsymbol{x},t)=\delta(\tau-T(\boldsymbol{x},t))\cdot\delta(\boldsymbol{v}-\boldsymbol{u}(\boldsymbol{x},t))$, where T and $\boldsymbol{u}$ are realizations of the fields, and τ and $\boldsymbol{v}$ are the corresponding sample-space variables.
- Deriving the fine-grained PDF and making use of the basic equations (1) for T and $\boldsymbol{u}$ leads to an evolution equation for $\hat{f}(\tau,\boldsymbol{v};\boldsymbol{x},t)$:

$$\frac{\partial}{\partial t}\hat{f}+\boldsymbol{u}\cdot\nabla\hat{f}=-\frac{\partial}{\partial\tau}\left[\Delta T\hat{f}\right]-\nabla_{\boldsymbol{v}}\cdot\left[\left(-\nabla p+\mathrm{Pr}\Delta\boldsymbol{u}+\mathrm{Pr}\,\mathrm{Ra}\,T\boldsymbol{e}_z\right)\hat{f}\right] \tag{3}$$

- Ensemble-averaging over realizations of T and $\boldsymbol{u}$ and exploiting homogeneity and isotropy gives an evolution equation for the full PDF $\tilde{f}(\tau,v_h,v_z;z)=2\pi v_h\left\langle\hat{f}(\tau,\boldsymbol{v};\boldsymbol{x},t)\right\rangle$:

$$v_z\frac{\partial}{\partial z}\tilde{f}=-\frac{\partial}{\partial\tau}\left[\Theta\tilde{f}\right]-\mathrm{Pr}\,\mathrm{Ra}\,\tau\frac{\partial}{\partial v_z}\tilde{f}-\frac{\partial}{\partial v_h}\left[\left(\Pi_h+\mathrm{Pr}\Lambda_h\right)\tilde{f}\right]-\frac{\partial}{\partial v_z}\left[\left(\Pi_z+\mathrm{Pr}\Lambda_z\right)\tilde{f}\right] \tag{4}$$

Here, the following conditional averages have been introduced, where the dependencies are in part abbreviated as $\star\hat{=}\tau,v_h,v_z,z$:

$$\langle\mathrm{Pr}\,\mathrm{Ra}\,T\boldsymbol{e}_z|\tau,v_h,v_z,z\rangle=\quad\mathrm{Pr}\,\mathrm{Ra}\,\tau\boldsymbol{e}_z$$
$$\langle\Delta T|\tau,v_h,v_z,z\rangle=:\;\Theta(\tau,v_h,v_z)$$
$$\langle-\nabla p|\tau,v_h,v_z,z\rangle=\langle-\hat{\boldsymbol{u}}_h\cdot\nabla p|\star\rangle\cdot\hat{\boldsymbol{v}}_h+\langle-\hat{\boldsymbol{u}}_z\cdot\nabla p|\star\rangle\cdot\hat{\boldsymbol{v}}_z$$
$$=:\;\Pi_h(\star)\cdot\hat{\boldsymbol{v}}_h+\Pi_z(\star)\cdot\hat{\boldsymbol{v}}_z$$
$$\langle\Delta\boldsymbol{u}|\tau,v_h,v_z,z\rangle=\langle\hat{\boldsymbol{u}}_h\cdot\Delta\boldsymbol{u}|\star\rangle\cdot\hat{\boldsymbol{v}}_h+\langle\hat{\boldsymbol{u}}_z\cdot\Delta\boldsymbol{u}|\star\rangle\cdot\hat{\boldsymbol{v}}_z$$
$$=:\;\Lambda_h(\star)\cdot\hat{\boldsymbol{v}}_h+\Lambda_z(\star)\cdot\hat{\boldsymbol{v}}_z$$

Temperature PDF And Method Of Characteristics

- Considering the temperature only, one can project (4) onto the temperature part and derive an evolution equation determining the temperature PDF $h(\tau;z)$:

$$\frac{\partial}{\partial z}\left[\langle u_z|\tau,z\rangle h\right]=-\frac{\partial}{\partial\tau}\left[\langle\Delta T|\tau,z\rangle h\right] \tag{5}$$

Thus, the temperature PDF is determined by the conditionally averaged vertical velocity and heat diffusion.
- Utilizing the method of characteristics, one can find trajectories $(\tau(s),z(s))$ in τ,z–phase space along which the PDE (5) transforms into an ODE.

Temperature PDF And Method Of Characteristics (contd.)

- The trajectories are parametrized by s, which can be identified as the time, and are definied by

$$\frac{\mathrm{d}}{\mathrm{d}s}\tau(s)=\langle\Delta T|\tau,z\rangle\Big|_{\substack{\tau=\tau(s)\\ z=z(s)}},\quad\frac{\mathrm{d}}{\mathrm{d}s}z(s)=\langle u_z|\tau,z\rangle\Big|_{\substack{\tau=\tau(s)\\ z=z(s)}} \tag{6}$$

- The resulting ODE can be integrated along trajectories, yielding

$$h(s)=h(s_0)\exp\left[-\int_{s_0}^{s}\mathrm{d}s\left(\frac{\partial}{\partial\tau}\langle\Delta T|\tau,z\rangle+\frac{\partial}{\partial z}\langle u_z|\tau,z\rangle\right)_{\substack{\tau(s)\\ z(s)}}\right] \tag{7}$$

This equation describes the temperature PDF at point $(\tau(s),z(s))$, evolving along the trajectory starting at $(\tau(s_0),z(s_0))$ in phase space.

Numerics: PDF And Conditional Averages

- Numerical simulations have been conducted for $\mathrm{Ra}=2.4\cdot10^7$, $\mathrm{Pr}=1$ and $\Gamma=4$. The Nusselt number is estimated to $\mathrm{Nu}=20.22$, the Reynolds number is $\mathrm{Re}=\frac{h\boldsymbol{u}_{\mathrm{rms}}}{\nu}=1038$.
- The two conditional averages in (6) that determine the trajectories are estimated from the numerics. They are plotted as a vector field $\left(\frac{\mathrm{d}\tau}{\mathrm{d}s},\frac{\mathrm{d}z}{\mathrm{d}s}\right)$ together with the color-coded temperature PDF $h(\tau;z)$:

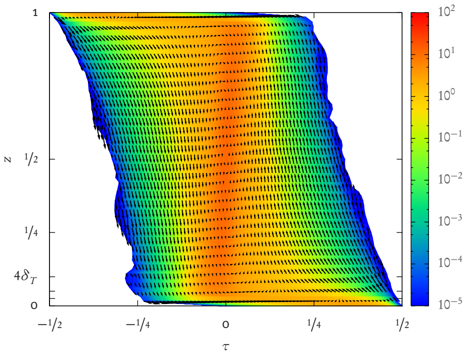

- Tracing the vector field in this graph, one can qualitatively reconstruct the trajectories and thus the typical *Rayleigh-Bénard cycle* of fluid heating up at the bottom, rising up, cooling down at the top plate, falling down and heating up again [14,15].
- Note for example that very hot fluid rises up quickly. This does not contribute much to the heat transport though, because these events occur rarely. Quantitative analysis of this will be done in the future.

Conclusions And Future Work

- The Lundgren-Monin-Novikov hierarchy and symmetry considerations allow us to derive equations determining PDFs.
- To estimate unclosed terms (i.e. conditional averages) from numerical simulations, volume penalization has been adapted to the Rayleigh-Bénard system.
- The evolution equation for the joint PDF of temperature and velocity is derived and the form of the conditionally averaged quantities is shown.
- Utilizing the method of characteristics, DNS is used to estimate the PDF and conditional averages for the temperature case, which can be used to reproduce the Rayleigh-Bénard cycle in a qualitative manner.
- The qualitative form and interpretation of the trajectories that determine the evolution in τ,z–phase space are given; a quantitative evaluation of the integral expression (7) is the next key point.
- We focused on the temperature PDF. An analogue treatment of the joint PDF is feasible, though the phase space has a higher dimensionality and is harder to visualize and to interpret.

References

[1] K. Schneider. *Computers & Fluids*, 34(10):1223–1238, 2005
[2] G.H. Keetels, U. D'Ortona, W. Kramer, H.J.H. Clercx, K. Schneider and G.J.F. van Heijst. *J. Comp. Phys.*, 227(2), 919–945, 2007
[3] T.Y. Hou and R. Li. *J. Comp. Phys.*, 226(1):379–397, 2007
[4] C. Shu and S. Osher. *J. Comp. Phys.*, 77(2):439–471, 1988
[5] *www.fftw.org*
[6] B. Kadoch. Transport and mixing in homogeneous and confined turbulent flows. *PhD thesis, Université de Provence*, 2009
[7] M. Sinhuber. *Diploma thesis, Westfälische Wilhelms-Universität Münster*, 2011
[8] *www.voreen.org*
[9] G.K. Batchelor. The theory of homogeneous turbulence. *Cambridge Science Classics*, 2001
[10] T.S. Lundgren. *Physics of Fluids*, 10(5):969–975, 1967
[11] A.S. Monin. *Prikl. Mat. Mekh.*, 31(6):1057–1068, 1967
[12] E.A. Novikov. *Soviet Physics-Doklady*, 12(11):1006–1008, 1967
[13] M. Wilczek and R. Friedrich. *Phys. Rev. E*, 80:016316, 2009
[14] J. Lülff, M. Wilczek and R. Friedrich. *New J. Phys.*, 13:015002, 2011
[15] J. Lülff. *Diploma thesis, Westfälische Wilhelms-Universität Münster*, 2011